

Depth-related Variability of Biological Nitrogen Fixation and Diazotrophic Communities in Mangrove Sediments

Zhiwen Luo

Sun Yat-Sen University School of Environmental Science and Engineering <https://orcid.org/0000-0002-5454-6733>

Qiuping Zhong

Sun Yat-Sen University

Xingguo Han

Swiss Federal Institute of Technology: Eidgenössische Technische Hochschule Zurich

Ruiwen Hu

Sun Yat-Sen University

Xingyu Liu

Sun Yat-Sen University

Weiming Huang

Sun Yat-Sen University

Zhengyuan Zhou

Sun Yat-Sen University

Wei Zhuang

Sun Yat-Sen University

Qingyun Yan

Sun Yat-Sen University

Zhili He

Sun Yat-Sen University

Cheng Wang (✉ wangcheng5@mail.sysu.edu.cn)

Environmental Microbiomics Research Center, School of Environmental Science and Engineering, Southern Marine Science and Engineering Guangdong Laboratory (Zhuhai), Sun Yat-sen University, Guangzhou 510006, China <https://orcid.org/0000-0002-3712-9890>

Research

Keywords: diazotroph, nitrogen fixation rate, depth-related variability, nitrogen cycling, adaptation strategy

Posted Date: March 1st, 2021

DOI: <https://doi.org/10.21203/rs.3.rs-262160/v1>

License:  This work is licensed under a Creative Commons Attribution 4.0 International License.

[Read Full License](#)

Abstract

Background: Nitrogen-fixing microorganisms (diazotrophs) provide biological available nitrogen and play a pivotal role in nitrogen cycling of mangrove sediments. However, most studies on diazotrophs have been restricted to easily accessible surface sediments, while the diversity, structure and ecological function of diazotrophic communities at the in-depth profile of mangrove sediments are largely unknown. Here, we investigated how biological nitrogen fixation vary with depth of mangrove sediments from the perspective of both NFR and diazotrophic communities.

Results: Through acetylene reduction assay, *nifH* gene amplicon and metagenomic sequencing, we found that the nitrogen fixation rate (NFR) increased but the diversity of diazotrophic community decreased with the depth of mangrove sediments. The structure of diazotrophic communities at different depths was largely driven by salinity, and exhibited a clear divergence at the partition depth of 50 cm. *Agrobacterium* and *Azotobacter* were specifically enriched at 50-100 cm sediments, while aerobic diazotrophs such as *Methylobacter* had a higher abundance at 0-30 cm. Consistent with the higher NFR, metagenomic analysis indicated the elevated abundance of nitrogen fixation genes (*nifH/D/K*) in deeper sediment layers, where nitrification genes (*amoA/B/C*) and denitrification genes (*nirK* and *norB*) became less abundant. Three metagenome-assembled genomes (MAGs) of diazotrophs from deep mangrove sediments indicated their facultative anaerobic and amphitrophic lifestyles as they contained genes for low-oxygen-dependent metabolism, hydrogenotrophic respiration, carbon fixation and pyruvate fermentation.

Conclusions: Together, this study determines the depth-related variability of NFR and diazotrophs, which potentially contribute to nitrogen sinks and relieve nitrogen limitation, especially in the deep sediments of mangrove ecosystems.

Background

Mangroves are highly productive ecosystems with immense ecological values [1]. Their high productivity is greatly attributed to the high nitrogen-fixing activity of diazotrophs in the mangrove sediments, which contribute about 40%-60% of the total nitrogen required by the mangrove ecosystem [2, 3]. However, due to tidal fluctuations and high denitrification rates, mangrove ecosystems are considered nitrogen-limited [4]. It has been determined that nitrogen fixation can primarily affect the nutrient status of sediments, since its products are the main source of nitrogen inputs in mangrove ecosystems [4, 5]. Therefore, as the rate-limiting step of nitrogen cycling, nitrogen fixation is particularly important to alleviate the nitrogen limitation of mangrove ecosystems [6, 7].

Diazotrophic communities are biological engines to drive the atmosphere nitrogen into mangrove ecosystems [8]. The diversity of diazotrophs is dependent on the climate, vegetation types and environmental properties across different ecosystems [9]. In terrestrial ecosystems, proteobacterial members are the prevalent diazotrophs with a high phylogenetic diversity, and exhibit preference for

gathering in specific habitats [10]. Taking alphaproteobacterial diazotroph as an example, *Azospirillum*, *Rhodobacter*, *Rhizobium* and *Bradyrhizobium* prefer the habitats with warm climate and relatively large precipitation, such as paddy soil and eastern Inner Mongolia steppe [9, 11]. Consistent with terrestrial ecosystems, the structure of marine diazotrophic communities also varies with environmental properties. For example, the cyanobacterium UCYN-A is broadly distributed in marine pelagic water and has a relative high biological NFR [12]. In contrast, anaerobic diazotrophs such as *Chlorobium* and *Desulfovibrio* prefer low temperature and appear uncommon in the surface ocean, but are preponderant in cold waters, especially in the Arctic [13]. Distinguishing from terrestrial and marine ecosystems, mangrove ecosystems act as the junctions between ocean and land, and specific diazotrophs are expected in such tidal swamp ecosystems. Although few studies have shown that sulfate-reducing bacteria may be the main nitrogen fixation group in mangroves [14], a systematic understanding of the diversity and ecological function of diazotrophic communities as well as their responses to environmental variations in the mangrove ecosystem is still lacking.

Our current understanding of diazotrophic community diversity and structure in the mangrove ecosystem is hitherto mainly limited to the surficial layers (i.e., 0–25 cm) of sediment columns, where the density of microorganisms is high [15, 16]. Yet, little is known about diazotrophic communities residing in the deeper (> 25 cm) sediment horizons. In fact, in-depth profiles of mangrove sediments have a gradient of resources and environmental properties, which have been identified as the universal factors directly or indirectly influencing the diazotrophic community in terrestrial ecosystems [17, 18]. For example, the sensitivity of diazotrophs to pH was different. *Bradyrhizobium* members often have higher acid resistance than other diazotrophs, while *Mesorhizobium* has a wider pH tolerant range with the optimal pH from 6 to 8 [19]. Anaerobic environments are more suitable for the survival of most diazotrophs, while aerobic diazotrophs need to evolve some mechanisms to protect nitrogenase from damages by oxygen [17, 20]. Ecological surveys further determine significant correlations of diazotrophic richness, diversity and community composition with soil moisture, C quality and quantity, N availability and the availability of trace elements (e.g., Mo, Fe and V) [18, 21]. These previous findings allow us to hypothesize that the deeper layers of mangrove sediments may contain diazotrophic communities that are specialized for their environments and fundamentally distinct from the surficial communities. Meanwhile, the in-depth profile of mangrove sediments provides a platform to investigate which physicochemical properties determine the depth-related distribution of diazotrophic communities in mangrove sediments.

From the view of ecological functions, biological nitrogen fixation not only provides reactional materials for downstream processes of the nitrogen cycle, but also is a key process to alleviate nitrogen limitation, especially in mangrove ecosystems [22, 23]. However, a central assumption of the progressive nitrogen limitation hypothesis is that, without changes in exogenous exchange of nitrogen in an ecosystem, increases in plant nitrogen uptake require increased soil nitrogen cycling rates [24]. This indicates that there exists a competition between plant nitrogen acquisition and microbiome-mediated nitrogen transformation processes [2, 25]. One reason for this competition is that the product of both nitrogen fixation and nitrate reduction (dissimilatory and assimilatory nitrate reduction to ammonium), NH_4^+ , not

only serves as the main form of nitrogen uptaken by mangrove roots, but also can be transformed by nitrification and ammonia assimilation [26, 27]. Therefore, nitrogen availability, driven by the balance among various nitrogen transformation processes, strongly regulates the ecological function of both terrestrial and aquatic ecosystems [28, 29]. Locating at the transition between land and ocean [30], mangroves are characterized by nitrogen limitation, but how the dynamic nitrogen transformation processes influence the extent of mangrove nitrogen limitation is still a vacancy. To fill this gap, we investigated the in-depth functional profile of the nitrogen transformation processes (e.g. nitrogen fixation and its downstream processes) in the mangrove ecosystem which is crucial for our better understanding of prevalent nitrogen limitation across wetlands.

In this study, we aimed to unveil how biological nitrogen fixation vary with depth of mangrove sediments and identify the key factors governing the in-depth profile of diazotrophic communities. In attempt to achieve these goals, we analyzed nitrogen fixation rate, diazotrophic communities and their key functional genes at 10 depths (0-100 cm) of mangrove sediments through the acetylene reduction assay, *nifH* gene amplicon sequencing and metagenome sequencing. We also constructed draft genomes of key nitrogen-fixing bacteria from these samples and determined potential metabolic pathways. This study reveals the depth-related variability of biological nitrogen fixation and diazotrophic communities in mangrove sediments, and advances our understanding of nitrogen limitation mechanisms in mangrove ecosystems.

Methods

Site description and sampling

The sampling site is located at the Qi'ao Mangrove Wetland Park (22°26'12.28" N, 113°38'26.12" E) of Guangdong province, China (Fig. S1), with a mean annual temperature of 22.4°C and the annual precipitation of 1700–2200 mm. The irregular semidiurnal tides are on average 0.17 and - 0.14 m of high and low tide levels, respectively. We collected sediment samples from the mangrove habitat, *Sonneratia apetala*, which is the dominant species in the Qi'ao Mangrove Wetland [31]. Three replicate sediment cores were collected in August 2019 using a 1-m long PVC sampling column. The sediment cores were sliced at 10 cm intervals into 10 depths (0–10, 10–20, 20–30, 30–40, 40–50, 50–60, 60–70, 70–80, 80–90, and 90–100 cm), yielding a total of 30 samples. The collected samples were stored in a portable cooler at 4°C and transported back to the laboratory within 24 h. Each collected sample was divided into two sub-samples: one was stored at 4°C for physicochemical property analysis, and the other was kept at - 80°C for DNA extraction.

Sediment physicochemical properties analysis

NFR was measured by acetelene reduction assay [32]. Briefly, fresh sediment (10.0 g) was put into a 120-mL serum vial. The vials were sealed with rubber stoppers and 10% of the headspace was replaced with pure and fresh acetylene (C₂H₂) before they were incubated in dark at 25°C. After incubation for 48 h, 200

μL headspace gas was taken out to measure the concentration of ethylene (C_2H_4) by Agilent gas chromatograph (HP7890B, Agilent, USA) equipped with a flame ionization detector and a HP-PLOT MoleSieve5A capillary column ($30.0\text{ m} \times 530\ \mu\text{m} \times 50\ \mu\text{m}$) (Agilent, USA), and He was used as a carrier gas [33].

Ammonia, nitrite and nitrate were determined by a multimode microplate reader (Varioskan LUX, Thermo Scientific, USA) after extraction from 2.0 g fresh samples with 2 M KCl. Fully digestion method was used to extract total ions and AB-DTAP extraction method was used to extract the available ions from 0.5 g air-dried sediments separately [34]. All of these trace element concentrations were determined by an inductively coupled plasma-optical emission spectrometer (ICP-OES, Avio 500, Perkin Elmer, Singapore). A sequential extraction protocol was used for ferrous and ferric ions from 0.5 g fresh sample [35], and iron content was measured by ICP-OES (Avio 500, Perkin Elmer, Singapore). Sediment moisture was measured by drying 10.0 g fresh sediments at 105°C to a constant weight. Sediment pH and salinity were measured with 2.0 g dry sediment in 1:2.5 (sediments/water) and 1:5 (sediments/water) suspension with a pH meter (SevenCompact210, Mettler-Toledo, USA) and a salinity meter (EUTECH SALT6+, Thermo Scientific, USA).

Sediment microbial community DNA extraction

The sediment microbial community DNA was extracted from 5.0 g sediment using a modified sodium dodecyl sulfate extraction method [36] combined with a Power Soil DNA Isolation Kit (Mo Bio Laboratories, Carlsbad, California, USA). The quality of sediment microbial community DNA was detected by NanoDrop ND-2000 Spectrophotometer (Thermo Fisher Scientific, MA, USA), and ratios of 260/280 and 260/230 were about 1.8 and above 1.7, respectively. DNA concentrations were quantified by a fluorescent method (Qubit 4 Fluorometer, Thermo Scientific, USA).

PCR amplification of *nifH* genes and amplicon sequencing

The *nifH* gene was amplified using the specific primer pair *PolF* (5'-TGCGAYCCSAARGCBGACTC-3') and *PolR* (5'-ATSGCCATCATYTCRCCGGA-3') with an expected fragment length of approximately 320 bp [37]. Both forward and reverse primers were tagged with an Illumina adapter sequence, a primer pad and a linker sequence. The reaction system for each sample was 50 μL , including 25 μL Phusion High-Fidelity DNA Polymerase (NEB, Inc., USA), 2 μL forward and reverse phasing primer, 5 μL DNA template and 16 μL RNase free Ultrapure water. The amplification was conducted in a BIO-RAD T100™ thermal cycler (Bio-Rad Laboratory, Hercules, USA) under the following conditions: initial denaturation at 94°C for 5 min, followed by 30 cycles of 94°C for 30 s, 55°C for 30 s and 72°C for 1 min, with a final extension at 72°C for 10 min. PCR products were then purified using AMPure XP Beads Kit (NEB, Inc., USA). Purified DNA was quantified by QuantiT™ dsDNA HS Reagent (Thermo Fisher Scientific, Inc., USA) and diluted to a concentration of 2 nM before sequencing. Paired-End *nifH* amplicon sequencing was performed using an Illumina HiSeq 2500 sequencer (Illumina, Inc., CA, USA) at Personalbio Biotechnology Co., Ltd. (Shanghai, China).

The quality filtering and pre-processing of raw sequences were performed on the Linux and Galaxy pipeline (<http://mem.rcees.ac.cn:8080/>). The primers were firstly eliminated by Cutadapt [38]. The low quality sequences (quality score < 20) were removed by Trimmomatic, and then forward and reverse reads were combined using FLASH [39]. Combined sequences of < 285 bp and > 350 bp were eliminated, and sequences contained one or more ambiguous base(s) ("N") were also removed. The chimeras were identified and eliminated using UCHIME [40]. Framebot software was used to correct potential frameshifts caused by sequencing errors [41], and only DNA sequences that covered > 30% of reference *nifH* protein translations were retained for further analysis. Operational taxonomic units (OTUs) were clustered at a 95% cutoff [42] of similarity level with protein reference sequences by using Quantitative Insights into Microbial Ecology (QIIME) implementation of UPARSE [43]. Taxonomic assignments for *nifH* OTUs were carried out an 80% [15] identity cut-off by searching representative sequences against reference *nifH* sequences with known taxonomic information.

Shotgun metagenome sequencing and data analysis

For surficial (0–10 cm), middle (50–60 cm), and deep (90–100 cm) sediment samples, one microgram of DNA was used for metagenome sequencing library preparations combined with NEBNext® Ultra™ DNA Library Prep Kit for Illumina (NEB, USA) as recommended by the manufacturer. Index codes were added to attribute sequences to each sample. The samples were purified (AMPure XP system), and the libraries were checked using Agilent 2100 Bioanalyzer (Agilent Technologies, CA) and quantified using real-time quantitative PCR. After cluster generation was performed on a cBot Cluster Generation System, paired-end reads (PE150) were performed on the Illumina platform. Low-quality (quality score ≤ 38 ; base N > 10 bp; the overlap length between adapter and reads > 15 bp) paired-end reads were filtered. The metagenomic assembly was performed using Megahit at default mode [44]. For assembled metagenomes, MetaGeneMark v.2.10. A non-redundant gene catalog (Unigenes) was built using CD-HIT v.4.5.8 to predict open reading frames [45]. Functional annotation was performed using DIAMOND combined with the Kyoto Encyclopedia of Genes and Genomes (KEGG) (<http://www.genome.jp/kegg/pathway.html>) database, and the KOs (KEGG Orthology) were divided into higher KEGG categories and KEGG pathways. Gene abundances were normalized into transcripts per-million (TPM) counts. The TPM values could be applied to metagenomes to remove the effects of total read counts and gene lengths when comparing the abundances of genes between samples [46].

Metagenomic binning and metagenome assembled genome (MAG) annotation

Genome assembly and binning were performed according to the MetaWRAP pipeline [47]. The sequences were assembled with MEGAHIT (options: -mink 21 -maxk 141 -step 12) [44] to generate contigs. Genome binning of assembled contigs were done using MetaBAT2 [48] and MaxBin2 [49], and the resulting bins were consolidated with the Bin_refinement module. The consolidated bin sets were further improved by the Reassemble_bins module to generate MAGs. The quality of MAGs was evaluated with CheckM (v1.0.5; Table S8). MAGs were analyzed further if their completeness were more than 50% and their contaminations were below 10% (Supplementary Data 1). The abundance of each MAG was expressed

as genome copies per million reads and calculated with Salmon [50]. Taxonomic assignments of MAGs were performed using the GTDB-Tk [51]. Gene prediction for MAGs was performed using prodigal (V2.6.2, default settings), and the predicted genes were further annotated using KAAS (KEGG Automatic Annotation Server) [52]. Additionally, we utilized a custom hmmer as well as the Pfam and TIGRFAM databases to search for key metabolic marker genes using hmmsearch and custom bit-score cutoffs [53].

Statistical analysis

Relationships between physicochemical characteristics, depth, diversity indices and relative abundance of diazotrophic communities were performed by linear regression analysis with GraphPad Prism (version 7.0). The other statistical analyses were conducted using R packages including vegan and ggplot2 (R Foundation for Statistical Computing, Vienna, Austria). The diazotrophic community dissimilarity based on Bray-Curtis distance matrices were evaluated by permutational multivariate analysis of variance (ADONIS) and analysis of similarities (ANOSIM). The contribution of environmental characteristics to diazotrophic community structure based on the Bray-Curtis distance matrices were assessed by analysis of variance (ANOVA). Additionally, we performed pairwise comparisons the functional genes involved in the nitrogen cycle of three selected sediment samples using STAMP (parameters: Fisher's exact test, Asymptotic-CC, Benjamini-Hochberg FDR), and screened out the functional genes with significant differences ($p < 0.05$).

We constructed structural equation model (SEM) to determine the direct and indirect contributions of sediment physicochemical properties, sediment depths, diazotrophic community richness and structure, to the in-depth profile of NFR. Sediment moisture and salinity were chosen in SEM, since both of them were identified as the significant predictors of the diazotrophic community structure based on the redundancy analysis (RDA). SEM can partition direct and indirect effects that one variable might have on another, estimate and compare the strengths of multiple effects, and ultimately provide mechanistic information on the drivers of diazotrophic communities and NFR [54]. SEM analysis was performed via the robust maximum likelihood evaluation method using AMOS 22.0 (AMOS IBM, USA). The SEM fitness was evaluated on the basis of a non-significant chi-square test ($P > 0.05$), the goodness-of-fit index (GFI), the comparative fit index (CFI), and the root mean square error of approximation (RMSEA).

Results

In-depth profile of NFR and physicochemical characteristics in mangrove sediments

We determined the NFR of 10 depths of the mangrove sediments using acetylene reduction assay (Additional file: Fig. S2). The NFR fluctuated in the range of 0-0.20 nmol/(g*h), and the average NFR was 0.031 nmol/(g*h). Clearly, we observed a depth-related variability of NFR, which reached a maximum at the depth of 90-100cm. Compared to the surficial layers (0–50 cm), the deeper layers (50–100 cm)

showed higher NFR and a significantly ($R^2 = 0.42$, $p < 0.05$) positive correlation between NFR and depth was detected in mangrove sediments, as revealed by a linear regression analysis (Fig. 1a).

In-depth profile of physicochemical characteristics was also examined in mangrove sediments. Salinity in mangrove sediments ranged from 0.43‰ to 1.54‰, and increased with depth (Additional file: Fig. S2, S3). Conversely, moisture of sediments, with an average of 52%, showed a consistent decreasing with depth (Additional file: Fig. S2, S3). pH and total iron concentration decreased from 0 cm to 50 cm, and then increased from 50 cm to 100 cm (Additional file: Fig. S3). However, the concentrations of NH_4^+ , NO_2^- , NO_3^- , available Fe and Fe^{3+} exhibited no momentous differences with depth (Additional file: Fig. S3). The linear regression analysis showed that moisture had a negative correlation with depth ($R^2 = 0.61$, $p < 0.05$) (Additional file: Fig. S3d), but salinity had a positive correlation with depth ($R^2 = 0.93$, $p < 0.0001$) (Additional file: Fig. S3f). It is expected that such changes of physicochemical properties may influence the in-depth profile of diazotrophic communities in mangrove sediments.

In-depth profile of diazotrophic communities in mangrove sediments

To investigate biotic factors contributing to the increased NFR with depth, we analyzed diazotrophic communities in mangrove sediments by sequencing *nifH* gene amplicons. From all samples, we obtained a total of 2,253,352 high-quality *nifH* sequences, and the *nifH* sequences were assigned into 974 operational taxonomic units (OTUs) and 59 genera after trimming (Additional file: Table S1). Notably, we observed the in-depth variation of diazotrophic communities in mangrove sediments. Both Shannon and Chao1 indices showed significant ($R^2 = 0.47$, $p < 0.05$) negative relationships with depth (Fig. 1a), highlighting the decrease of diazotrophic community diversity and richness with depth. Meanwhile, diazotrophic diversity indices showed negative relationships with NFR (Fig. 1b), namely, diazotrophic community diversity and richness decreased with the increasing of depth. Furthermore, principal coordinates analysis (PCoA) showed that diazotrophic microbial communities in mangrove sediments were well separated by depth, and 50 cm was identified as the partitioning depth based on the Bray-Curtis distance (Additional file: Fig. S4). Two nonparametric tests (ANOSIM and ADONIS) further verified such significant variations ($p < 0.001$) of diazotrophic communities between sediment layers above and below 50 cm. Together, these findings determined the reduced diversity and varied structure of diazotrophic communities with depth of mangrove sediments.

Key diazotrophs contributing to increased NFR with depth

Taxonomic analysis of diazotrophic communities showed that bacteria (92.53%) dominated biological nitrogen fixation in mangrove sediments, and a few archaea (such as *Methanomicrobia* belong to *Euryarchaeota*) (0.18%) had the potential to fix nitrogen. At the phylum level, *Proteobacteria* was prevalent diazotrophs in mangrove sediments, which is consistent with terrestrial ecosystems [42]. Among *Proteobacteria*, *Deltaproteobacteria* occupied the largest proportion with an average relative abundance of 31%, followed by *Gammaproteobacteria* and *Alphaproteobacteria* (Additional file: Fig.

S5a). At the genus level, aerobic diazotrophs such as *Methylomonas* and *Heliobacterium* had higher relative abundances in the surficial layers (0–50 cm), while diazotrophic members represented by *Agrobacterium*, *Desulfuromonas*, *Klebsiella* and *Azospira* had higher relative abundances in the deeper layers (50–100 cm) (Additional file: Fig. S5b).

We performed Linear discriminant analysis Effect Size (LEfSe) on diazotrophic communities in mangrove sediments. Interestingly, diazotrophs presented manifest hierarchical clustering when 50 cm was set as the partitioning depth (Additional file: Fig. S6). The LEfSe results showed that, most of the diazotrophs enriched in surficial sediments (above 50 cm) belonged to *Proteobacteria*, such as *Burkholderiales*, *Nitrosomonadales*, *Desulfarculales*, *Myxococcales* and *Methylococcales*. Conversely, *Agrobacterium* affiliated to *Alphaproteobacteria*, *Azotobacter* affiliated to *Deltaproteobacteria*, and *Dehalococcoides* affiliated to *Chloroflexi* appeared conspicuous clustering in sediments below 50 cm (Additional file: Fig. S6). The diazotrophs specific for deep sediments tended to be crucial for biological nitrogen fixation in mangrove sediments because their higher relative abundances in deeper sediments corresponded with stronger NFR (Fig. 2b).

To further examine whether these deep sediment-specific diazotrophs played major roles in biological nitrogen fixation, we performed Pearson's correlation analysis between NFR and abundances of diazotrophic genera in mangrove sediment profiles (Fig. 2, Additional file: Table S2). Among 11 diazotrophic genera having negative correlations with NFR, *Desulfovibrio* ($R^2 = 0.56$, $p < 0.05$) and *Anaeromyxobacter* ($R^2 = 0.53$, $p < 0.05$) had higher relative abundances, accounting for 5.2% and 2.9% of all diazotrophs, respectively (Fig. 2b, Additional file: Table S3). However, we also observed two diazotrophic genera that have positive correlations with NFR, namely *Agrobacterium* ($R^2 = 0.73$, $p < 0.05$) and *Azotobacter* ($R^2 = 0.48$, $p < 0.05$) (Fig. 2b). *Azotobacter* had a higher average relative abundance (11.9%) than *Agrobacterium* (3.3%) (Additional file: Table S3). Given their positive correlations with depth and their functional roles previously reported [4, 55], we assumed that both of them (especially *Azotobacter*) played a decisive role for the increased NFR with depth of mangrove sediments.

Relationships among sediment physicochemical characteristics, diazotrophic communities and NFR

To reveal the relationship between diazotrophic communities and environmental factors, we performed RDA to estimate the factors that had significant ($p < 0.01$) influences on diazotrophic communities (Fig. 3a). The results showed that nitrate, ammonia, moisture and salinity were the important driving factors of diazotrophic communities in mangrove sediments. Specially, moisture and salinity were the only two environmental characteristics significantly related to depth (Additional file: Fig. S3d, f). Through all detected depths, Pearson's correlation analysis revealed that diazotrophic communities in terms of Chao 1 index and PCoA1 of diazotrophic communities were significantly ($p < 0.05$) negative with salinity (Additional file: Table S4, S5), suggesting that salinity and moisture were the main environmental factors driving the in-depth variation of diazotrophic communities in mangrove sediments.

To further evaluate the direct and indirect effects of depth, sediment properties (including moisture and salinity), and diazotrophic community richness and structure on NFR, we conducted SEM analysis based on known relationships among these observed variables (Fig. 3b). Consistent with the linear regression (Additional file: Fig. S3d, f) and RDA results (Fig. 3a), depth showed a directly positive effect on salinity and a directly negative effect on moisture, and salinity exerted significant effects on the diazotrophic community structure (Fig. 3a). Among all the observed variables in the model, only the diazotrophic community structure had a direct effect on NFR (Fig. 3c) although depth could indirectly influence NFR by strongly affecting sediment salinity (Fig. 3b). Collectively, these results indicated that salinity-driven diazotrophic community structure played a critical role in determining the in-depth profile of NFR in mangrove sediments.

In-depth profile of biological nitrogen fixation and its downstream processes in mangrove sediments

Samples from three depths (M1: 0–10 cm, M2: 50–60 cm, M3: 90–100 cm) of mangrove sediments were selected for metagenomic sequencing analysis of N-cycling gene profiles across the surficial, middle and deep sediments. We first proposed an in-depth schema to illustrate metabolic potentials for various nitrogen cycling processes based on key N-cycling functional genes (Fig. 4a-c). Notably, a total of eight pathways consistently revealed depth-related variations in terms of functional gene abundances (Fisher's exact test, $p < 0.05$), including nitrogen fixation, nitrification, denitrification, dissimilatory nitrate reduction to ammonium (DNRA), assimilatory nitrate reduction, ammonia assimilation, nitrate assimilation and organic N decomposition.

Consistent with the trend of diazotrophic activity (NFR), the gene clusters for nitrogen fixing (*nifH/D/K*) increased in abundance with depth. Compared to the surficial layer (M1: 0–10 cm), the abundance of nitrogen fixation genes in deep sediment increased by 41.9% (Fig. 4c). Such increasing trend also occurred in ammonia assimilation and assimilatory nitrate reduction (Fig. 4). Particularly, the functional genes (*nasA*, *narB* and *nirA*) involved in assimilatory nitrate reduction remarkably increased 1.5, 17.6 and 9.3 times from the surficial layer to the deep sediment (Fig. 4c). By contrast, the abundance of functional genes involved in nitrification (*aomA*, *amoB*, *amoC* and *hao*), denitrification (*nirK*, *nirS*, *norB* and *norC*), DNRA (*nrfA*, *nrfH*, *nirB* and *nirD*) and organic N decomposition (*ureA*, *ureB* and *ureC*) significantly ($p < 0.05$) decreased with depth (Fig. 4). Taking the rate-limiting process of denitrification as example, the abundance of *napA/B* decreased by 21.5% from the surficial layer to the deep sediment (Fig. 4c). Overall, these functional gene patterns showed that both biological nitrogen fixation and its downstream processes in mangrove sediments underwent the depth-related variation with divergent trends.

Versatile functions and adaptation strategies of diazotrophic MAGs

De novo assembly and binning of metagenomic sequencing data from three depths of mangrove sediments allowed the reconstruction of 3 archaeal and 64 bacterial MAGs (completeness > 50%, contaminated < 10%; Additional file: Supplementary Data 1). Given that metagenomic sequencing

generated enormous data accompanied by tremendous undiscovered information, we inferred their potential physiological capabilities by annotating genes using the KAAS and TIFRFAM databases. Among all 67 high-quality and high-completion MAGs, three MAGs possessed genes for nitrogen fixation (*nifH/D/K*), namely M2.bin.35, M2.bin.46 and M3.bin.42, which represented one *Chloroflexi* and two *Desulfurmonadales* (Fig. 5, Additional file: Supplementary Data 2). Interestingly, these three MAGs consistently contained genes associated with other nitrogen cycling processes, such as ammonia assimilation and the complete DNRA pathway (Fig. 5, Additional file: Supplementary Data 2). Additionally, M2.bin.35 had the genes involved with entire denitrification except for converting NO_3^- to N_2O (Fig. 5, Additional file: Supplementary Data 2). However, genes related to nitrate assimilation, assimilatory nitrate reduction, organic N decomposition or nitrification were absent in these three diazotrophic MAGs (Fig. 5, Additional file: Supplementary Data 2).

Further functional annotation showed many potentials of these diazotrophic MAGs. From the perspective of energy metabolism, three MAGs contained genes involved in the complete or nearly complete carbon fixation pathways (such as Wood-Ljungdahl pathway) (Fig. 5, Additional file: Supplementary Data 2), so they would have the potential to convert inorganic carbon into organic molecules such as acetyl-CoA. Via TCA cycle, acetyl-CoA could be further utilized by these diazotrophs to generate energy for microbial metabolism (Fig. 5, Additional file: Supplementary Data 2). Combined with the detection of genes encoding lactate dehydrogenase (*ldh*), pyruvate oxidoreductase (*porA/C*) and formate dehydrogenase (*fodG*) (Fig. 5, Additional file: Supplementary Data 2), our results suggest that these diazotrophs showed an amphitrophic lifestyle in mangrove sediments. From the perspective of adaptive strategies, diazotrophs from middle or deep mangrove sediments contained NiFe-hydrogenase genes for anaerobic respiration, oxidative stress responses (*hyaB*, *hybC*), sulfur reduction and anaerobic cobalamin biosynthesis (Fig. 5, Additional file: Supplementary Data 2). The adaptation of diazotrophs to the low-oxygen deep sediments was further supported by the occurrence of genes related to pyruvate oxidoreductase (*porA/C*), thioredoxin peroxidase, cytochrome c oxidases (*coxA/B*), *ccb*₃-type cytochrome c oxidases (*ccoN/O/P/Q*) and a cytochrome bd ubiquinol oxidase (*cydA*) (Fig. 5, Additional file: Supplementary Data 2). More importantly, we also observed that these diazotrophic MAGs contained glycine betaine reductase and glucose/sorbosone dehydrogenase to support their adaptation to hypersaline deep sediments. Together, these results indicated that the halotolerant diazotrophs in deep mangrove sediments were functionally versatile and facultative anaerobes.

Discussion

Mangroves are considered as typical nitrogen-limited ecosystems [56]. Characterizing the biological nitrogen fixation and diazotrophic communities is, therefore, crucial to fully elucidate the nutrient status and ecological functions of mangrove ecosystems. In this study, we systematically examined the in-depth profile of NFR and diazotrophic communities across 10 depths of mangrove sediments. A prominent finding is that the diversity of diazotrophic communities decreased whereas NFR increased with the increase of sediment depth. Such depth-related variability of biological nitrogen fixation could be further

supported by our metagenomic sequencing analysis, which revealed an elevated abundance of genes related to biological nitrogen fixation in deeper sediments. Moreover, the metagenomic binning and functional annotation of diazotrophic MAGs provide a genetic evidence for the functional versatility and adaptive strategies of diazotrophs under the low-oxygen and oligotrophic conditions of deeper sediments. These results provide novel insights into the depth-related variability of NFR and diazotrophic communities, and advance our understanding of the relationship between biological nitrogen fixation and nitrogen limitation in mangrove ecosystems.

Our in-depth survey of mangrove sediments revealed a clear divergence of diazotrophic community composition at the partition depth of 50 cm. Although the diversity of diazotrophic communities was lower in deep sediments than in surface ones, the deep sediment-specific diazotrophs, including *Agrobacterium* and *Azotobacter*, contributed to a higher NFR in deep sediments. There are two main reasons for this observation. First, the lifestyle of diazotrophs was related to nitrogen fixation efficiency. Previous studies found that microaerophilic and anaerobic diazotrophs often exhibited a higher nitrogen fixation efficiency than aerobic diazotrophs [57]. In our study, the dominant diazotroph in the deep sediment was *Agrobacterium* sp., which has been reported to be a typical facultative anaerobe with the capability of anaerobic respiration in the presence of nitrate [58]. In line with this opinion, our MAG annotation indicated many genes related to low oxygen-dependent pathways, and determined a facultative anaerobic lifestyle of diazotrophs in deep mangrove sediments. Thus, the deep layer of mangrove sediments with lower oxygen concentrations could provide suitable conditions for microaerophilic/anaerobic diazotrophs to efficiently fix nitrogen [59], which is well consistent with high NFR in the deep sediment. Second, decreasing oxygen and ammonium concentrations with depth may facilitate to ensure the high activity of nitrogenase. It has been reported that metalloproteins of nitrogenase were extremely sensitive to oxygen and irreversibly destroyed under high oxygen conditions [60]. For example, the activity of MoFe protein and Fe protein in *Azotobacter* was reduced in a few minutes when they were exposed to air [61]. Besides, high ammonium concentrations were well known to inhibit nitrogenase synthesis through regulating the transcription of *nifA* [55]. When exposed to high ammonium concentrations, the protein *NifL* in *Azotobacter* could inhibit the activity of *nifA*, and subsequently result in the inactivation of nitrogenase [62]. These findings suggest that under the fluctuated physicochemical gradients, the changes of nitrogenase activity and diazotrophic communities jointly contribute to the in-depth variability of biological nitrogen fixation in the mangrove sediment.

Located at the transition between ocean and land, mangrove sediments experienced the tidal fluctuation day after day [63]. Probably due to the continuous scouring of surficial sediments by tides and the deposition of salinity in depth [64, 65], a continuous increase of salinity with depth of mangrove sediments was observed in our study. More interestingly, in agreement with the paddy soil [66] and salt marsh [67], salinity was identified as the most important environmental filter for shaping the diazotrophic community structure in mangrove sediments, as revealed by our RDA and SEM results. Such niche partition of diazotrophs across sediment depths may be closely tied to their salt tolerance and associated strategies. In the deep sediment layers with high salinity, we observed that the diazotrophic community was dominated by *Azotobacter* and *Agrobacterium*, which belong to more-salt-tolerant diazotrophs [68,

69] and tend to replace less-salt-tolerant ones in deep sediments [70]. Moreover, these diazotrophs thriving in high-salinity sediments potentially apply the “low-salt-in” strategy to balance the osmotic potential of the cytoplasm [71]. This strategy was reported for accumulating low-molecular-weight organic compounds within the cell to maintain an osmotic equilibrium with the surrounding environment by excluding salt ions from the cytoplasm [72]. To support the adaptive strategy of diazotrophs to high salinity, we did observe that diazotrophic MAGs contained glycine betaine reductase and glucose/sorbosone dehydrogenase, which are well known osmolytes to balance the osmotic pressure created by the hypersaline habitat [73, 74]. Collectively, our study highlights the role of salinity in controlling the in-depth structure of the diazotrophic communities and indicates the putative strategy of diazotrophs for high salinity tolerance in mangrove sediments.

Under nitrogen limited conditions, the nitrogen partitioning between mangrove species and sediment microorganisms altered the extent of nitrogen limitation in mangrove ecosystems [24, 75]. Previous studies reported that mangrove species could acquire nitrogen from the sediments under both inorganic (nitrate and ammonium) and organic (e.g., urea, amino acid) forms [26, 76]. However, the uptake of ammonium and nitrate by plants was down regulated under carbon limiting conditions [77]. Therefore, in deep mangrove sediments with low organic carbon content [78], the main form of nitrogen uptaken by mangrove species was assumed to be amino acids. In support of this assumption, our metagenomic sequencing analysis showed that with the increasing depth of mangrove sediments, both biological nitrogen fixation and ammonia assimilation pathways were enhanced, whereas ammonia and organic nitrogen loss by denitrification and organic nitrogen decomposition pathways was weakened. These results indicate that there were probably more amino acids for mangroves to take up, thus relieving nitrogen limitation in the deep layer of mangrove sediments. As the balance between nitrogen cycling processes determined whether nitrogen sink or source is occurring in mangrove ecosystems [79], we also inferred that the notable variation of nitrogen cycling processes with depth would result in the increased organic nitrogen burial and decreased N_2O/N_2 emissions in deep sediments, which suggests a possible role of mangrove ecosystems as a potential nitrogen sink.

Conclusions

In summary, this study illustrates the depth-related variability of biological nitrogen fixation in mangrove sediments from the perspective of both NFR and diazotrophic communities. The diversity of diazotrophic communities decreased with depth of mangrove sediments, but the NFR and nitrogen fixation-related gene abundances increased. The salinity-driven structure of diazotrophic communities showed a clear divergence at the partition depth of 50 cm, and high abundances of *Azotobacter* and *Agrobacterium* at 50–100 cm sediments contributed to an elevation of NFR in deep mangrove sediments. Accompanied by such an elevation, our metagenomic sequencing analysis indicated that ammonia and organic nitrogen loss by denitrification and organic nitrogen decomposition pathways was weakened with depth. These in-depth variations in nitrogen fixation and its downstream processes indicated the mitigation of nitrogen limitation and a possible nitrogen sink in the deep layers of mangrove sediments. Overall, this study

provides new insights into comprehensive understanding of biological nitrogen fixation and its ecological functions in mangrove sediments.

Declarations

Author contributions

Z.W.L and C.W. conceived and designed the study. Z.W.L., Q.P.Z. and W.M.H. performed the laboratory work and detailed the sampling. Z.W.L., X.G.H., R.W.H., X.Y.L., Z.Y.Z. and W.Z. carried out the bioinformatics and statistical analysis. Z.W.L. and C.W. wrote the first draft of the manuscript. Z.W.L., C.W., Q.Y.Y. and Z.L.H discussed results and edited and wrote the paper. All authors read and approved the final version of the manuscript.

Funding

This study was supported by the National Natural Science Foundation of China (91951207, 52070196, 32000070, 41771095), the Guangdong Basic and Applied Basic Research Foundation (2019A1515011406), the Fundamental Research Funds for the Central Universities (19lgpy165, 19lgzd28, 19lgpy162), and the Hundred Talents Program through Sun Yat-sen University (38000-18841205, 99318-18841205, 38000-18821107).

Availability of data and materials

The nucleotide sequences and metagenomic data of microbial communities in mangrove sediments were deposited in SRA database under accession number PRJNA694572 and PRJNA698080. The authors declare that the primary data supporting the findings of this study are available within this article and in the additional files. Extra data supporting the findings of this study are available from the corresponding author upon request.

Ethics approval and consent to participate

This manuscript does not report data collected from humans or animals. Therefore, ethics approval and a consent to participate are not necessary.

Consent for publication

Not applicable.

Competing interests

The authors declare no competing interests.

References

1. Goldberg L, Lagomasino D, Thomas N, Fatoyinbo T. Global declines in human-driven mangrove loss. *Global Change Biol.* 2020;26(10):5844-5855.
2. Holguin G, Vazquez P, Bashan Y. The role of sediment microorganisms in the productivity, conservation, and rehabilitation of mangrove ecosystems: an overview. *Biol Fertility Soils.* 2001;33(4):265-278.
3. Zhuang W, Yu X, Hu R, Luo Z, Liu X, Zheng X, et al. Diversity, function and assembly of mangrove root-associated microbial communities at a continuous fine-scale. *npj Biofilms Microbi.* 2020;6(1):52.
4. Zhang Y, Dong J, Yang Z, Zhang S, Wang Y. Phylogenetic diversity of nitrogen-fixing bacteria in mangrove sediments assessed by PCR–denaturing gradient gel electrophoresis. *Arch Microbiol.* 2008;190(1):19.
5. Romero IC, Jacobson M, Fuhrman JA, Fogel M, Capone DG. Long-term nitrogen and phosphorus fertilization effects on N₂ fixation rates and *nifH* gene community patterns in mangrove sediments. *Mar Ecol-Evol Persp.* 2012;33(1):117-127.
6. Fernandes SO, Michotey VD, Guasco S, Bonin PC, Loka Bharathi PA. Denitrification prevails over anammox in tropical mangrove sediments (Goa, India). *Mar Environ Res.* 2012;74:9-19.
7. Tang W, Cerdán-García E, Berthelot H, Polyviou D, Wang S, Baylay A, et al. New insights into the distributions of nitrogen fixation and diazotrophs revealed by high-resolution sensing and sampling methods. *ISME J.* 2020;14(10):2514-2526.
8. Kuypers MMM, Marchant HK, Kartal B. The microbial nitrogen-cycling network. *Nat Rev Microbiol.* 2018;16(5):263-276.
9. Wang Y, Li C, Kou Y, Wang J, Tu B, Li H, et al. Soil pH is a major driver of soil diazotrophic community assembly in Qinghai-Tibet alpine meadows. *Soil Biol Biochem.* 2017;115:547-555.
10. Levy-Booth DJ, Prescott CE, Grayston SJ. Microbial functional genes involved in nitrogen fixation, nitrification and denitrification in forest ecosystems. *Soil Biol Biochem.* 2014;75:11-25.
11. Wan X, Gao Q, Zhao J, Feng J, van Nostrand JD, Yang Y, et al. Biogeographic patterns of microbial association networks in paddy soil within Eastern China. *Soil Biol Biochem.* 2020;142:107696.
12. Gradoville MR, Bombar D, Crump BC, Letelier RM, Zehr JP, White AE. Diversity and activity of nitrogen-fixing communities across ocean basins. *Limnol Oceanogr.* 2017;62(5):1895-1909.
13. Langlois RJ, Hümmer D, LaRoche J. Abundances and distributions of the dominant *nifH* phylotypes in the Northern Atlantic Ocean. *Appl Environ Microbiol.* 2008;74(6):1922-1931.

14. Liu X, Yang C, Yu X, Yu H, Zhuang W, Gu H, et al. Revealing structure and assembly for rhizophyte-endophyte diazotrophic community in mangrove ecosystem after introduced *Sonneratia apetala* and *Laguncularia racemosa*. *Sci Total Environ*. 2020;721:137807.
15. Yu X, Yang X, Wu Y, Peng Y, Yang T, Xiao F, et al. *Sonneratia apetala* introduction alters methane cycling microbial communities and increases methane emissions in mangrove ecosystems. *Soil Biol Biochem*. 2020;144:107775.
16. Lin X, Hetharua B, Lin L, Xu H, Zheng T, He Z, et al. Mangrove sediment microbiome: adaptive microbial assemblages and their routed biogeochemical processes in Yunxiao Mangrove National Nature Reserve, China. *Microb Ecol*. 2019;78(1):57-69.
17. Masuda T, Inomura K, Takahata N, Shiozaki T, Sano Y, Deutsch C, et al. Heterogeneous nitrogen fixation rates confer energetic advantage and expanded ecological niche of unicellular diazotroph populations. *Commun Biol*. 2020;3(1):172.
18. Hsu S-F, Buckley DH. Evidence for the functional significance of diazotroph community structure in soil. *ISME J*. 2009;3(1):124-136.
19. Laranjo M, Oliveira S. Tolerance of *Mesorhizobium* type strains to different environmental stresses. *Anton Leeuw*. 2011;99(3):651-662.
20. Stal LJ. The effect of oxygen concentration and temperature on nitrogenase activity in the heterocystous cyanobacterium *Fischerella* sp. *Sci Rep*. 2017;7(1):5402.
21. Singh BK, Tate K, Thomas N, Ross D, Singh J. Differential effect of afforestation on nitrogen-fixing and denitrifying communities and potential implications for nitrogen cycling. *Soil Biol Biochem*. 2011;43(7):1426-1433.
22. Omoregie EO, Crumbliss LL, Bebout BM, Zehr JP. Determination of nitrogen-fixing phylotypes in *Lyngbya* sp. and *Microcoleus chthonoplastes* cyanobacterial mats from Guerrero Negro, Baja California, Mexico. *Appl Environ Microbiol*. 2004;70(4):2119-2128.
23. Canfield DE, Glazer AN, Falkowski PG. The evolution and future of earth's nitrogen cycle. *Science*. 2010;330(6001):192-196.
24. Averill C, Rousk J, Hawkes C. Microbial-mediated redistribution of ecosystem nitrogen cycling can delay progressive nitrogen limitation. *Biogeochemistry*. 2015;126(1):11-23.
25. Moreau D, Bardgett RD, Finlay RD, Jones DL, Philippot L. A plant perspective on nitrogen cycling in the rhizosphere. *Funct Ecol*. 2019;33(4):540-552.
26. Miller AJ, Cramer MD. Root nitrogen acquisition and assimilation. *Plant Soil*. 2005;274(1):1-36.
27. Tu Q, He Z, Wu L, Xue K, Xie G, Chain P, et al. Metagenomic reconstruction of nitrogen cycling pathways in a CO₂-enriched grassland ecosystem. *Soil Biol Biochem*. 2017;106:99-108.
28. Russell DG, Warry FY, Cook PLM. The balance between nitrogen fixation and denitrification on vegetated and non-vegetated intertidal sediments. *Limnol Oceanogr*. 2016;61(6):2058-2075.
29. Reis CRG, Nardoto GB, Oliveira RS. Global overview on nitrogen dynamics in mangroves and consequences of increasing nitrogen availability for these systems. *Plant Soil*. 2017;410(1):1-19.

30. Li S, Meng X, Ge Z, Zhang L. Vulnerability assessment of the coastal mangrove ecosystems in Guangxi, China, to sea-level rise. *Reg Environ Change*. 2015;15(2):265-275.
31. Yu C, Feng J, Liu K, Wang G, Zhu Y, Chen H, et al. Changes of ecosystem carbon stock following the plantation of exotic mangrove *Sonneratia apetala* in Qi'ao Island, China. *Sci Total Environ*. 2020;717:137142.
32. Han L-L, Wang Q, Shen J-P, Di HJ, Wang J-T, Wei W-X, et al. Multiple factors drive the abundance and diversity of the diazotrophic community in typical farmland soils of China. *FEMS Microbiol Ecol*. 2019;95(8).
33. Das S, De TK. Microbial assay of N₂ fixation rate, a simple alternate for acetylene reduction assay. *MethodsX*. 2018;5:909-914.
34. Soltanpour PN, Workman S. Modification of the NH₄HCO₃-DTPA soil test to omit carbon black. *Commun Soil Sci Plant Anal*. 1979;10(11):1411-1420.
35. Cai C, Leu AO, Xie G-J, Guo J, Feng Y, Zhao J-X, et al. A methanotrophic archaeon couples anaerobic oxidation of methane to Fe(III) reduction. *ISME J*. 2018;12(8):1929-1939.
36. Zhou J, Bruns MA, Tiedje JM. DNA recovery from soils of diverse composition. *Appl Environ Microbiol*. 1996;62(2):316-322.
37. Poly F, Monrozier LJ, Bally R. Improvement in the RFLP procedure for studying the diversity of *nifH* genes in communities of nitrogen fixers in soil. *Res Microbiol*. 2001;152(1):95-103.
38. Martin M. Cutadapt removes adapter sequences from high-throughput sequencing reads. *EMBnet J*. 2011;17(1):3.
39. Magoč T, Salzberg SL. FLASH: fast length adjustment of short reads to improve genome assemblies. *Bioinformatics*. 2011;27(21):2957-2963.
40. Edgar RC, Haas BJ, Clemente JC, Quince C, Knight R. UCHIME improves sensitivity and speed of chimera detection. *Bioinformatics*. 2011;27(16):2194-2200.
41. Wang Q, Quensen JF, Fish JA, Lee TK, Sun YN, Tiedje JM, et al. Ecological patterns of *nifH* genes in four terrestrial climatic zones explored with targeted metagenomics using FrameBot, a new informatics tool. *mBio*. 2013;4(5):9.
42. Feng J, Penton CR, He Z, Van Nostrand JD, Yuan MM, Wu L, et al. Long-term warming in Alaska enlarges the diazotrophic community in deep soils. *mBio*. 2019;10(1):e02521-02518.
43. Edgar RC. UPARSE: highly accurate OTU sequences from microbial amplicon reads. *Nat Methods*. 2013;10(10):996-998.
44. Li D, Liu C-M, Luo R, Sadakane K, Lam T-W. MEGAHIT: an ultra-fast single-node solution for large and complex metagenomics assembly via succinct de Bruijn graph. *Bioinformatics*. 2015;31(10):1674-1676.
45. Fu L, Niu B, Zhu Z, Wu S, Li W. CD-HIT: accelerated for clustering the next-generation sequencing data. *Bioinformatics*. 2012;28(23):3150-3152.

46. Seyler LM, Trembath-Reichert E, Tully BJ, Huber JA. Time-series transcriptomics from cold, oxic subseafloor crustal fluids reveals a motile, mixotrophic microbial community. *ISME J.* 2020.
47. Uritskiy GV, DiRuggiero J, Taylor J. MetaWRAP - a flexible pipeline for genome-resolved metagenomic data analysis. *Microbiome.* 2018;6(1):158.
48. Kang DWD, Li F, Kirton E, Thomas A, Egan R, An H, et al. MetaBAT 2: an adaptive binning algorithm for robust and efficient genome reconstruction from metagenome assemblies. *Peerj.* 2019;7:13.
49. Wu Y-W, Simmons BA, Singer SW. MaxBin 2.0: an automated binning algorithm to recover genomes from multiple metagenomic datasets. *Bioinformatics.* 2015;32(4):605-607.
50. Patro R, Duggal G, Love MI, Irizarry RA, Kingsford C. Salmon provides fast and bias-aware quantification of transcript expression. *Nat Methods.* 2017;14(4):417-419.
51. Parks DH, Chuvochina M, Waite DW, Rinke C, Skarszewski A, Chaumeil P-A, et al. A standardized bacterial taxonomy based on genome phylogeny substantially revises the tree of life. *Nat Biotechnol.* 2018;36(10):996-1004.
52. Moriya Y, Itoh M, Okuda S, Yoshizawa AC, Kanehisa M. KAAS: an automatic genome annotation and pathway reconstruction server. *Nucleic Acids Res.* 2007;35(suppl_2):W182-W185.
53. Dombrowski N, Teske AP, Baker BJ. Expansive microbial metabolic versatility and biodiversity in dynamic Guaymas Basin hydrothermal sediments. *Nat Commun.* 2018;9(1):4999.
54. Chen L, Jiang Y, Liang C, Luo Y, Xu Q, Han C, et al. Competitive interaction with keystone taxa induced negative priming under biochar amendments. *Microbiome.* 2019;7(1):77.
55. Inomura K, Bragg J, Riemann L, Follows MJ. A quantitative model of nitrogen fixation in the presence of ammonium. *PLOS ONE.* 2018;13(11):e0208282.
56. Liao S, Wang Y, Liu H, Fan G, Sahu SK, Jin T, et al. Deciphering the microbial taxonomy and functionality of two diverse mangrove ecosystems and their potential abilities to produce bioactive compounds. *mSystems.* 2020;5(5):e00851-00819.
57. Smercina DN, Evans SE, Friesen ML, Tiemann LK. To fix or not to fix: controls on free-living nitrogen fixation in the rhizosphere. *Appl Environ Microbiol.* 2019;85(6):e02546-02518.
58. Lee BD, Ellis JT, Dodwell A, Eisenhauer EER, Saunders DL, Lee MH. Iodate and nitrate transformation by *Agrobacterium/Rhizobium* related strain DVZ35 isolated from contaminated Hanford groundwater. *J Hazard Mater.* 2018;350:19-26.
59. Zhang YY, Yang QS, Ling J, Van Nostrand JD, Shi Z, Zhou JZ, et al. Diversity and structure of diazotrophic communities in mangrove rhizosphere, revealed by high-throughput sequencing. *Front Microbiol.* 2017;8:11.
60. Dixon R, Kahn D. Genetic regulation of biological nitrogen fixation. *Nat Rev Microbiol.* 2004;2(8):621-631.
61. Robson RL, Postgate JR. Oxygen and hydrogen in biological nitrogen fixation. *Annu Rev Microbiol.* 1980;34:183-207.

62. Reyes-Ramirez F, Little R, Dixon R. Mutant forms of the *Azotobacter vinelandii* transcriptional activator *NifA* resistant to inhibition by the *NifL* regulatory protein. *J Bacteriol.* 2002;184(24):6777-6785.
63. Collins DS, Avdis A, Allison PA, Johnson HD, Hill J, Piggott MD, et al. Tidal dynamics and mangrove carbon sequestration during the Oligo–Miocene in the South China Sea. *Nat Commun.* 2017;8(1):15698.
64. Feng X, Xu S, Li J, Yang Y, Chen Q, Lyu H, et al. Molecular adaptation to salinity fluctuation in tropical intertidal environments of a mangrove tree *Sonneratia alba*. *BMC Plant Biol.* 2020;20(1):178.
65. Fu Z, Wang P, Sun J, Lu Z, Yang H, Liu J, et al. Composition, seasonal variation, and salinization characteristics of soil salinity in the Chenier Island of the Yellow River Delta. *Glob Ecol Conserv.* 2020;24:e01318.
66. Barua S, Tripathi S, Chakraborty A, Ghosh S, Chakrabarti K. Studies on non-symbiotic diazotrophic bacterial populations of coastal arable saline soils of India. *Indian J Microbiol.* 2011;51(3):369-376.
67. Severin I, Confurius-Guns V, Stal LJ. Effect of salinity on nitrogenase activity and composition of the active diazotrophic community in intertidal microbial mats. *Arch Microbiol.* 2012;194(6):483-491.
68. Yan J, Li Y, Yan H, Chen WF, Zhang X, Wang ET, et al. *Agrobacterium salinitolerans* sp. nov., a saline-alkaline-tolerant bacterium isolated from root nodule of *Sesbania cannabina*. *Int J Syst Evol Microbiol.* 2017;67(6):1906-1911.
69. Allam NG, Kinany R, El-Refai E, Ali WY. Potential use of beneficial salt tolerant bacteria for improving wheat productivity grown in salinized soil. *J Microbiol Res.* 2018;8(2):43-53.
70. Zhang K, Shi Y, Cui X, Yue P, Li K, Liu X, et al. Salinity is a key determinant for soil microbial communities in a desert ecosystem. *mSystems.* 2019;4(1):e00225-00218.
71. Oren A. Life at high salt concentrations, intracellular KCl concentrations, and acidic proteomes. *Front Microbiol.* 2013;4:315-315.
72. Gunde-Cimerman N, Plemenitaš A, Oren A. Strategies of adaptation of microorganisms of the three domains of life to high salt concentrations. *FEMS Microbiol Rev.* 2018;42(3):353-375.
73. Ahmed V, Verma MK, Gupta S, Mandhan V, Chauhan NS. Metagenomic profiling of soil microbes to mine salt stress tolerance genes. *Front Microbiol.* 2018;9(159).
74. Smith LT, Smith GM, Madkour MA. Osmoregulation in *Agrobacterium tumefaciens*: accumulation of a novel disaccharide is controlled by osmotic strength and glycine betaine. *J Bacteriol.* 1990;172(12):6849-6855.
75. Liu Q, Qiao N, Xu X, Xin X, Han JY, Tian Y, et al. Nitrogen acquisition by plants and microorganisms in a temperate grassland. *Sci Rep.* 2016;6(1):22642.
76. Hachiya T, Sakakibara H. Interactions between nitrate and ammonium in their uptake, allocation, assimilation, and signaling in plants. *J Exp Bot.* 2016;68(10):2501-2512.
77. Van Oosten MJ, Di Stasio E, Cirillo V, Silletti S, Ventorino V, Pepe O, et al. Root inoculation with *Azotobacter chroococcum* 76A enhances tomato plants adaptation to salt stress under low N

conditions. BMC Plant Biol. 2018;18(1):205.

78. Zhang M, Luo Y, Lin La, Lin X, Hetharua B, Zhao W, et al. Molecular and stable isotopic evidence for the occurrence of nitrite-dependent anaerobic methane-oxidizing bacteria in the mangrove sediment of Zhangjiang Estuary, China. Appl Microbiol Biotechnol. 2018;102(5):2441-2454.
79. Hussein AH, Rabenhorst MC. Modeling of nitrogen sequestration in coastal marsh soils. Soil Sci Soc Am J. 2002;66(1):324-330.

Figures

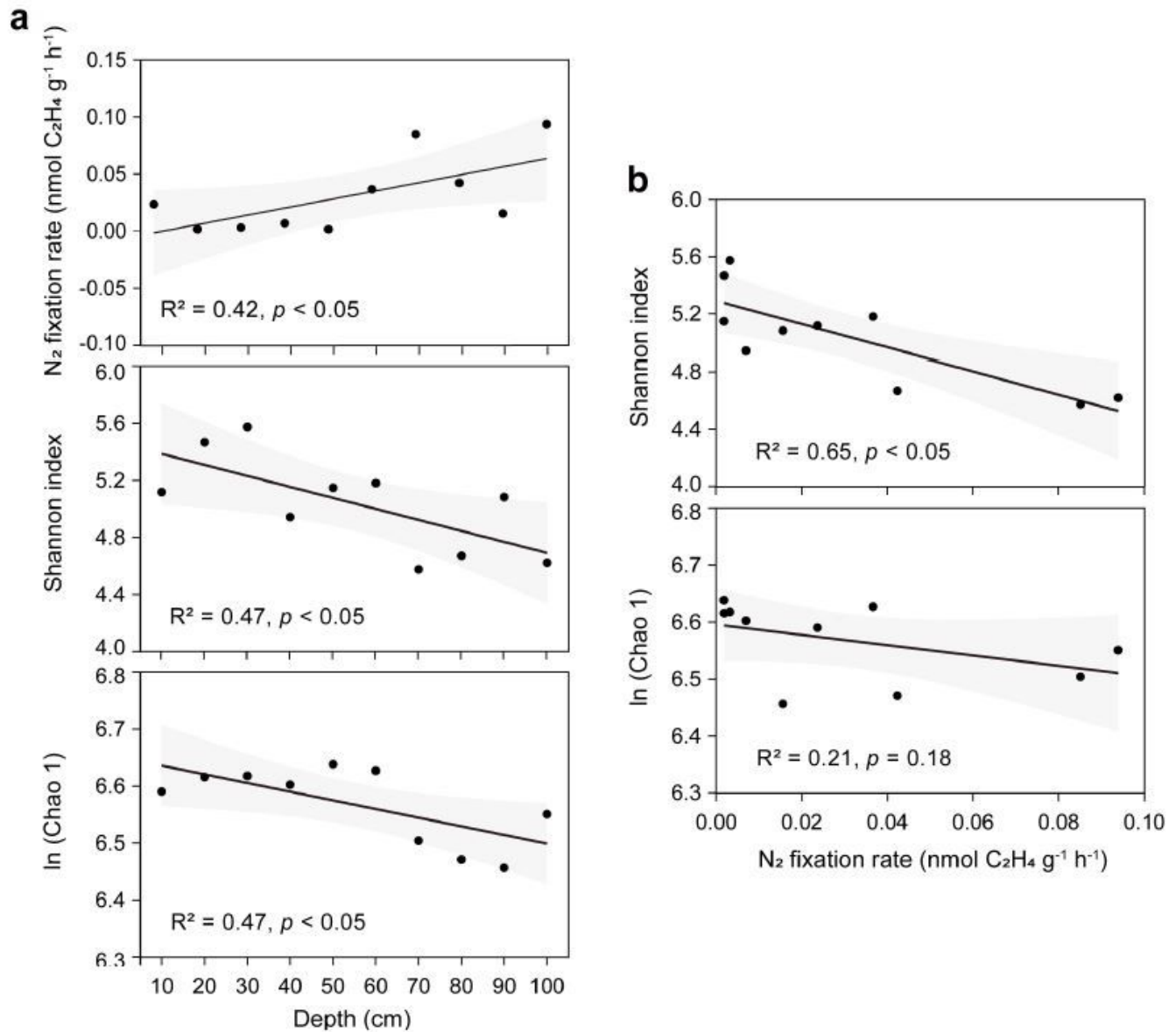


Figure 1

and grey shaded areas represent linear regressions and 95% confidence intervals, respectively. R2 was obtained by linear regression analysis and p was obtained by Pearson's correlation analysis.

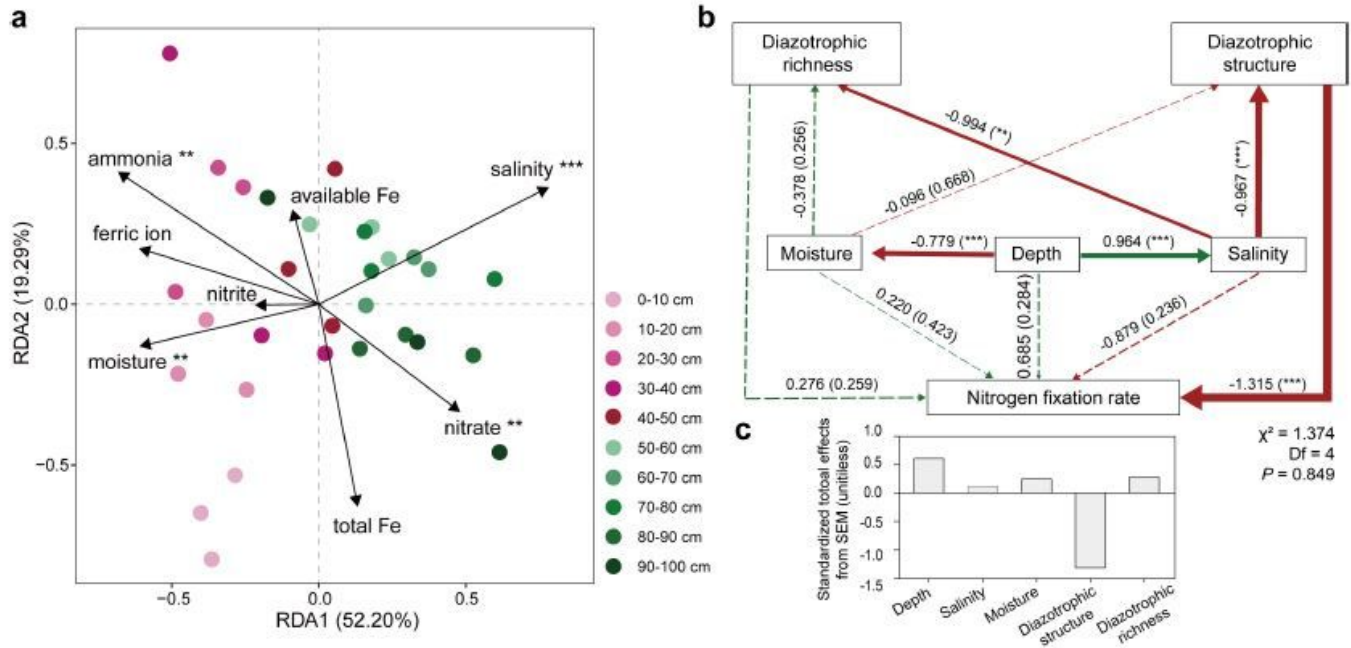


Figure 3

Relationships between sediment properties and diazotrophic communities. a. Redundancy analysis (RDA) showed the environmental drivers of diazotrophic communities. b. Structural equation modeling (SEM) of direct and indirect effects of depth, sediment properties (moisture and salinity) and molecular attributes (diazotrophic community diversity and structure) on NFR. The hypothetical model fits our data well as suggested by the goodness-of-fit statistics: Chi-square = 1.374, degrees of freedom = 4, probability level = 0.849, GFI = 0.951, CFI = 1.000, RMSEA = 0.000. Arrows indicate the hypothesized direction of causation, green arrows indicate positive relationships, and red arrows indicate negative relationships. Solid lines represent significant correlations, and dashed lines indicate insignificant correlations. The numbers adjacent to arrows are standardized path coefficients proportional to thickness of the lines, with p values in the brackets. c. Standardized total effects (the sum of direct plus indirect effects from SEM) of the major factors on NFR. **: $0.001 \leq p \leq 0.01$; ***: $p \leq 0.001$.

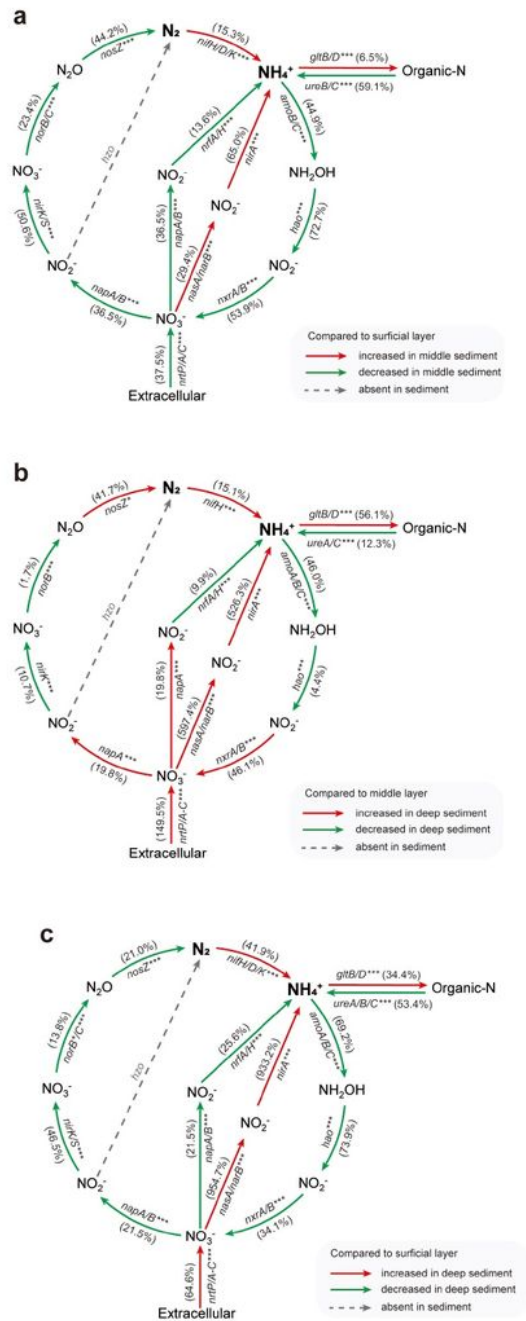


Figure 4

In-depth gene profile of nitrogen cycling processes in mangrove sediments. a-c. The shifts in functional gene abundance when the surficial layer was compared with the middle sediment (a), the middle layer with the deep sediment (b), and the surficial layer with the deep sediment (c). Arrows indicate the direction of reaction. Red arrows indicate that the abundance of genes increased from the surficial layer to the deeper sediment, and green indicate a decreasing trend. The genes adjacent to arrows are

representative functional genes for each process, and the numbers in the brackets are percentages increased or decreased in gene abundance. *: $0.01 \leq p \leq 0.05$; **: $0.001 \leq p \leq 0.01$; ***: $p \leq 0.001$.

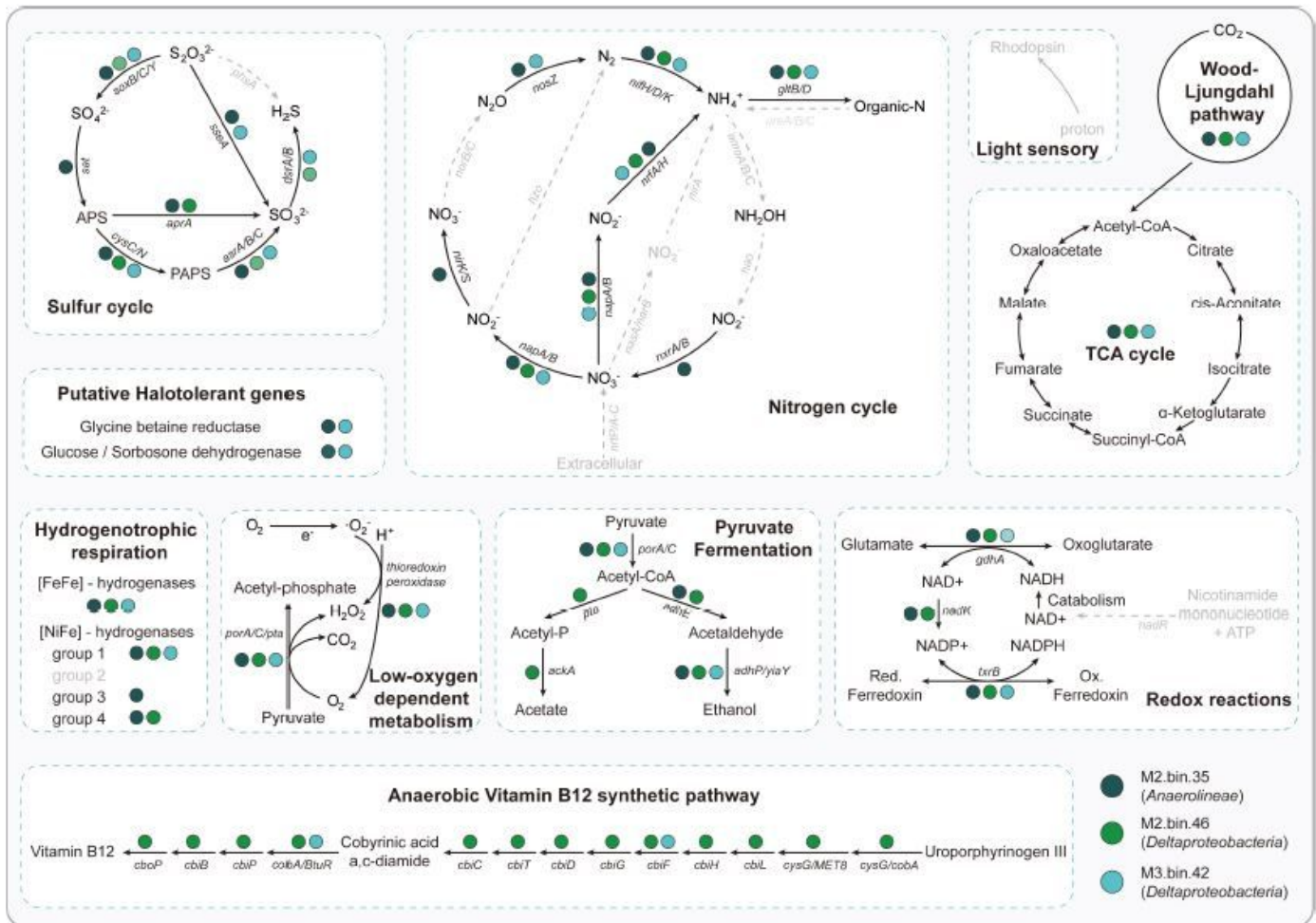


Figure 5

Metabolic characteristics of three key diazotrophs projected on key pathways in mangrove sediments. Dark green: metagenome-assembled genomes (MAGs) belonging to M2.bin.35 (Anaerolineae). Light green: MAGs belonging to M2.bin.46 (Deltaproteobacteria). Light blue: MAGs belonging to M3.bin.42 (Deltaproteobacteria). Black solid arrows indicate the genes/pathways that MAGs possessed, and grey dashed arrows indicate the missing genes/pathways. A detailed list of genes in these three key diazotrophs can be found in Additional file: Supplementary Data 2.

Supplementary Files

This is a list of supplementary files associated with this preprint. Click to download.

- [Additionalfile1.pdf](#)
- [Additionalfile2.xlsx](#)

- [Additionalfile3.xlsx](#)